Inducing $\mathbb{Z}_2$ topology in twisted nodal superconductors

Kevin P. Lucht [1], Pavel A. Volkov [2,3] and J. H. Pixley [1,4]

[1]*Department of Physics and Astronomy, Center for Materials Theory, Rutgers University, Piscataway, New Jersey 08854, USA*
[2]*Department of Physics, Harvard University, Cambridge, Massachusetts 02138, USA*
[3]*Department of Physics, University of Connecticut, Storrs, Connecticut 06269, USA*
[4]*Center for Computational Quantum Physics, Flatiron Institute, 162 5th Avenue, New York, New York 10010, USA*

(Received 13 February 2024; revised 15 April 2024; accepted 22 April 2024; published 6 May 2024)

Twisted nodal superconductors have been shown to exhibit chiral topological superconductivity under broken time-reversal symmetry. Here we show how a time-reversal preserving topological superconductivity can be induced in nodal triplet superconductor multilayers. For a bilayer system, the application of a Josephson spin current in triplet superconductors induces a nonzero spin Chern number per node in momentum space. However, we show that stabilizing a nontrivial global $\mathbb{Z}_2$ invariant requires an odd number of layers. As a specific example, we consider trilayers with three forms of twist: chiral, alternating, and single-layer. For chiral and single-layer case, we find that a gap opening in the dispersion leads to a nontrivial $\mathbb{Z}_2$ topological invariant. For single-layer twists, we show how this invariant is nontrivial when extended to an arbitrary odd number of layers.

DOI: 10.1103/PhysRevB.109.184507

I. INTRODUCTION

Twisted nodal superconductors are a promising platform to realize topological superconductivity through the spontaneous or the induced formation of a chiral order parameter [1–3]. Of potential superconducting candidate materials, $Bi_2Sr_2CaCu_2O_{8+\delta}$ (BSCCO) has received considerable attention due to its highly two-dimensional (2D) structure, remaining superconducting even in the limit of a single layer (comprising two CuO_2 planes) with a similar transition temperature as in its bulk counterpart [4]. Although twisted bilayers have not been realized, twisted flakes have been achieved leading to the observation of time-reversal symmetry breaking (TRSB) interfacial superconductivity [5–8]. As experimental techniques advance, various forms of stacked and twisted cuprates from one to several layers with the necessary nodal structure are a plausible achievement in the near future. Beyond twisted cuprates, other layered systems have been predicted theoretically to exhibit topological characteristics. Some of these predictions include chiral superconductivity using layered triplet superconductors [9–11], heterobilayers with higher order topology [12], or effective triplet superconductors formed via singlet superconductors [13].

The focus of the bulk of the proposals above has been using TRSB to form $\mathbb{Z}$ topological superconductors (classified as class C or D in the Atland-Zirnbauer (AZ) classification [14]). However, in 2D, time-reversal invariant (TRI) topological superconductors can exist with a $\mathbb{Z}_2$ index for class DIII [15–18]. TRI topological superconductors have been of theoretical interest in part due to their analog to the quantum spin hall state of TRI topological insulators. Furthermore, TRI topological superconductors host a pair of helical edge modes which are characterized as a Kramers' pair of Majorana fermions. This pair can also form around TRI defects and manifest as an emergent supersymmetry [16], and as bound states in junction devices which can be controlled for quantum information processing [19]. For class DIII superconductors, the TRI state is mainly reserved to triplet superconductors as a singlet order parameter preserves the SU(2) spin symmetry. However, various proximity effect arrangements [20–22] or external fields [23] can yield a TRI topological phase without the need for a triplet superconductor.

In analogy to previous work on chiral topological superconductivity [2], we will explore here the possibility to induce $\mathbb{Z}_2$ superconductivity in twisted nodal superconductors by external perturbations that preserve time-reversal symmetry. In particular, spin current is one such perturbation that will be a major focus of the following manuscript.

Spin currents in superconducting systems have been studied for their potential utility in spintronic applications [24], with most of the works focusing on heterostructures involving magnetic materials (primarily ferromagnets) and singlet superconductors [25,26] or Rashba spin-orbit coupling [27,28]. For triplet superconductors, theoretical studies have shown that spin currents, including nondissipative (Josephson) ones, are related to misalignment of the d-vector of the order parameters [29,30].

In this work, we demonstrate a strategy to create time-reversal preserving $\mathbb{Z}_2$ topological superconductors in twisted multilayers of triplet nodal superconductors. In particular, we show that a Josephson spin current creates a misalignment between the d-vectors of the layers leading to the opening of a topological gap in the spectrum which is characterized by a spin Chern number. The total spin Chern number of the system forms a $\mathbb{Z}_2$ invariant and we show that it can be nontrival only for systems with an odd number of layers. As an explicit example, we use a three layer system (that we extend to N layers) to show how the topological character depends on the twisting arrangement, which is no longer unique beyond a pair of layers. We focus on three common twisting arrangements displayed in Fig. 1: where the twist angle between nearest neighboring layers is constant and with the same sign dubbed

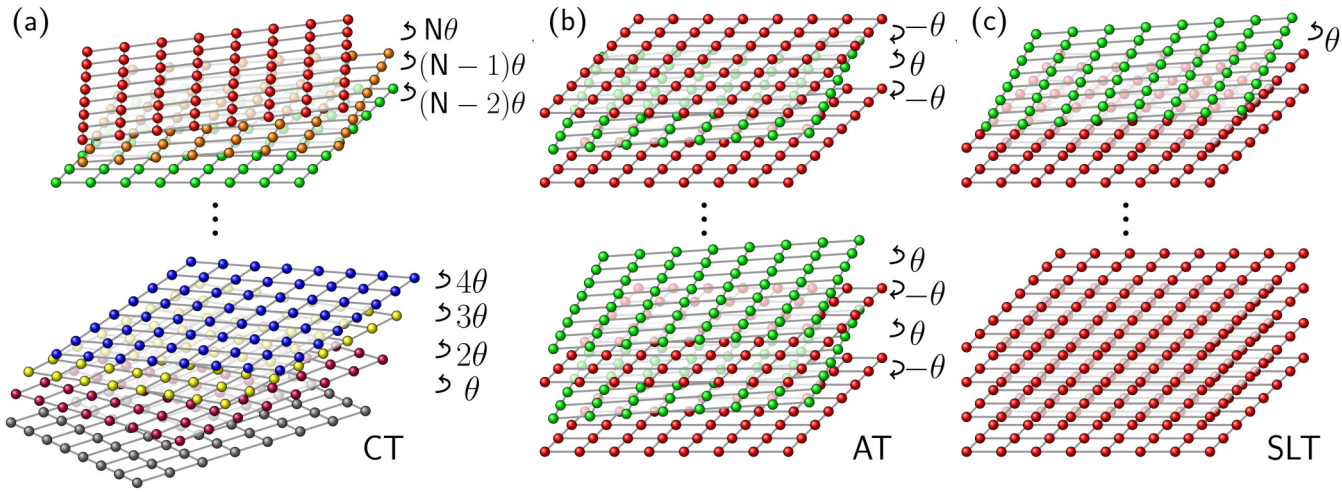

FIG. 1. Twisting arrangements for N-layered systems. At the top of each twisting arrangement is the $N = 3$ layered case which are extended below to arbitrary N. The arrow indicates the direction a given layer is rotated by an angle θ. (a) displays chiral twists (CTs) where each layer n is rotated by angle $n\theta$ to form continually rotated layers with a fixed orientation. (b) displays an alternating twists (ATs) where odd layers are rotated by angle θ and even layers by $-\theta$. (c) displays a single-layer twist (SLT) arrangement where layer N is rotated at an angle θ while the remaining $N - 1$ layers are not twisted.

chiral twists (CT) or with an alternating sign called alternating twists (AT) and where only the top layer is twisted with the remaining layers untwisted that we have dubbed single-layer twists (SLTs) and is the main focus of the present work. While the case of AT is topologically trivial [31], for the CT and SLT systems with an odd number of layers, a topological gap is formed with a nontrivial topological index. Focusing on the SLTs for a three layer system, we explicitly show in a small twist angle model how to compute the $\mathbb{Z}_2$ index, and then extend this to an arbitrary number of layers to show its stability with an odd number of layers.

The proceeding manuscript is organized as follows: in Sec. II, we examine the topological classification of a general superconducting Hamiltonian and perturbations of a N-layered system. We attribute one of these perturbations to a spin Josephson effect which is explored in Sec. III using a two layered system which leads to a trivial topological invariant. Section IV extends this spin Josephson effect to a three layered system to show that in combination with their arrangement has a nontrivial topological invariant. We conclude with Sec. V and comment on the topological invariant in a general N-layered system and its connection to 2.5-dimensional (2.5-D) systems [32].

II. SYMMETRY CLASSIFICATION OF CONTINUUM MODEL

To identify in general what twisted superconductors are topological, we utilize the Cartan symmetry classifications focusing on the superconducting Altland-Zirnbauer (AZ) symmetry classes. To realize $\mathbb{Z}_2$ topology, we have to extend the single-layer classification of 2D superconductors to an N-layered system, and then identify perturbations which allow for the formation of a TRI $\mathbb{Z}_2$ topological superconductor for layered systems. In this extension, we will first ignore the influence of twist angle, and then introduce contributions from arbitrary small twist angles between layers.

The second quantized Hamiltonian for a N-layered system in the continuum can be written as

$$\mathcal{H} = \sum_{\mathbf{k}} \Psi_{\mathbf{k}}^{\dagger} H_N(\mathbf{k}) \Psi_{\mathbf{k}}, \tag{1}$$

where we use Balian-Werthammer (B-W) spinors $\Psi_{\mathbf{k}}^{\dagger} = (\Psi_{\mathbf{k},1}^{\dagger}, \Psi_{\mathbf{k},2}^{\dagger}, \ldots, \Psi_{\mathbf{k},N}^{\dagger})$ and $\Psi_{\mathbf{k},l}^{\dagger} = (c_{\mathbf{k},\uparrow,l}^{\dagger}, c_{\mathbf{k},\downarrow,l}^{\dagger}, c_{-\mathbf{k},\uparrow,l}, c_{-\mathbf{k},\downarrow,l})$ for each layer $l = 1, 2, \ldots, N$. This Hamiltonian describes a single valley where the momenta $\mathbf{k}$ are local to a Bogoliubov-de Gennes (BdG) Dirac node positioned at $\mathbf{K}_N$ such that $\mathbf{k} = \mathbf{K} - \mathbf{K}_N$ where $\mathbf{K}$ is an arbitrary momenta. The Bloch Hamiltonian will be constructed in terms of $h_0(\mathbf{k})$ which is a single-layer component with no twist local (in k space) to the Dirac node centered at K_N expressed as

$$h_0(\mathbf{k}) = \xi \tau_3 s_0 + \delta \hat{\Delta}(\mathbf{k}), \tag{2}$$

where $\xi = v_F k_{\parallel}$, $\delta = v_{\Delta} k_{\perp}$, τ_i is the Nambu basis, and s_i is the spin basis. The parameters v_F is the velocity of the normal dispersion and v_{Δ} is the "velocity" of the order parameter, and $k_{\parallel}$ is the momenta parallel to K_N and $k_{\perp}$ is the momenta perpendicular to K_N. Local to the node at $\mathbf{K}_N$, $k_{\parallel}$ and $k_{\perp}$ forms an orthogonal coordinate system (see Fig. 2). For our purposes, we consider the order parameter $\hat{\Delta}(\mathbf{k})$ to be expressed as

$$\hat{\Delta}_s = s_2 \tau_2 \tag{3}$$

or

$$\hat{\Delta}_t(\mathbf{k}) = (\mathbf{d}(\mathbf{K}_N) \cdot \mathbf{s})(i s_2)\tau_1, \tag{4}$$

which are singlet and triplet order parameters, respectively. Without loss of generality, we will chose the d-vector of the form $\mathbf{d}(\mathbf{K}_N) = (d_1(\mathbf{K}_N), 0, 0)$ where $d_1(\mathbf{K}_N) = -d_1(-\mathbf{K}_N)$ and $|d_1(\mathbf{K}_N)| = 1$.

Treating the tunneling only between nearest neighboring layers and identical between each layer, a general untwisted

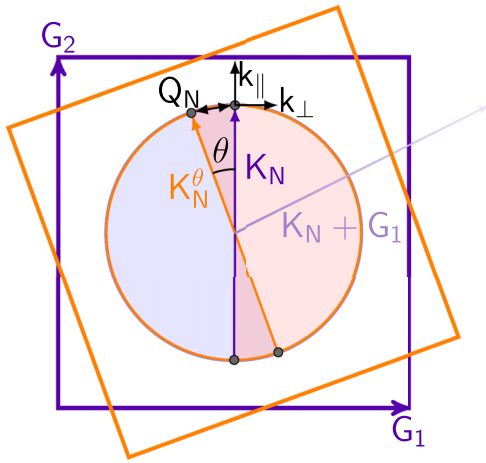

FIG. 2. An overview of the Brillouin zone of a twisted interface with circular Fermi surfaces. The interior color represents the sign of the superconducting order parameter with line of zeros displayed as orange and purple. The intersection of the line of gap zeros with the Fermi surface (black circles) depict the Dirac nodes. The nonrotated layer in purple has reciprocal lattice vectors $\mathbf{G}_1$ and $\mathbf{G}_2$ and node positioned at $\mathbf{K}_N$. From $\mathbf{K}_N$, a local coordinate system is constructed. When the top layer in orange is rotated by an angle θ, its node positioned at $\mathbf{K}_N^\theta$ introduces a displacement vector $\mathbf{Q}_N$ along $k_\perp$. Higher order tunneling represented by the fading vector $\mathbf{K}_N + \mathbf{G}_1$ are neglected.

N layer Hamiltonian can be written as

$$H_N(\mathbf{k}) = \begin{pmatrix} h_0(\mathbf{k}) & T(\mathbf{k}) & 0 & \\ T^*(\mathbf{k}) & h_0(\mathbf{k}) & T(\mathbf{k}) & \cdots \\ 0 & T^*(\mathbf{k}) & h_0(\mathbf{k}) & \\ & \vdots & & \ddots \end{pmatrix}, \tag{5}$$

where the off-diagonal interlayer tunneling matrix $T(\mathbf{k})$ is represented in terms of bases τ_i and s_j. We will now address the affect of introducing a small twist of angle $\pm\theta$ to an arbitrary layer n. The twist translates this layer's node by introducing a displacement $\mathbf{Q}_N$ along $k_\perp$ as shown in Fig. 2 (for more details see Ref. [10]). This affects the tunneling matrix by involving both the untwisted momentum components $\mathbf{k}$ and twisted momentum $\mathbf{k}' = \mathbf{k}^\theta$ such that $T(\mathbf{k}) \to T(\mathbf{k}, \mathbf{k}') \approx T(\mathbf{k} - \mathbf{k}')$ and

$$T(\mathbf{k} - \mathbf{k}') = t_{\mathbf{k},\mathbf{k}'} \tau_i s_j, \tag{6}$$

where $t_{\mathbf{k},\mathbf{k}'}$ is the Fourier transformed tunneling strength. Treating the tunneling strength as local in k-space to the node $\mathbf{K}_N$, and neglecting momenta beyond the initial Brillouin zone as shown in Fig. 2 as T falls off exponentially in this regime [10], the tunneling strength can therefore be simplified to

$$t_{\mathbf{k},\mathbf{k}'} \approx \frac{t_{\mathbf{K}_N}}{\Omega} \equiv t, \tag{7}$$

where $t_{\mathbf{K}_N}$ is the tunneling strength at the node $\mathbf{K}_N$ and Ω is the unit cell area of a layer (for technical details of this approximation, see Ref. [10]). Furthermore, the displacement also contributes a term $H_{tw,n}(\mathbf{k})$ which is added to the twisted layer's Hamiltonian of Eq. (2)

$$H_{tw,n}(\mathbf{k}) = \pm\alpha t \hat{\Delta}(\mathbf{k}), \tag{8}$$

where $\alpha = \frac{v_\Delta Q_N}{t}$ and the subscript n is the layer index where the twist is applied.

We now aim to classify the Hamiltonian under the discrete symmetry operators for time reversal $\mathcal{T} = U_T K$ and charge conjugation $\mathcal{C} = U_C K$, where $U_{T,C}$ are unitary operators. As the contributions of twist do not affect the classification of the Hamiltonian in Eq. (5), they are neglected. These operators realize the $\mathcal{T}$ and $\mathcal{C}$ symmetries of the Hamiltonian as

$$U_T^\dagger H_N^*(\mathbf{k}) U_T = H_N(-\mathbf{k}), \; U_C^\dagger H_N^*(\mathbf{k}) U_C = -H_N(-\mathbf{k}). \tag{9}$$

It is important to note that $H_N(\mathbf{k})$ represents a single valley centered at $\mathbf{K}_N$ and these discrete operations relate this valley to another located at $-\mathbf{K}_N$. Since $H_N(\mathbf{k})$ can be decomposed into single-layer components, we can likewise decompose the unitary operators U_T and U_C in Eq. (9) as a direct sum

$$U_{T/C} = U_{1,T/C}^{(1)} \oplus U_{1,T/C}^{(2)} \oplus \cdots \oplus U_{1,T/C}^{(N)}, \tag{10}$$

where the superscript corresponds to the layer index and $U_{1,T/C}$ is the unitary operator for time reversal/charge conjugation corresponding to the single-layer Hamiltonian such that

$$U_{1,T}^\dagger h_0^*(\mathbf{k}) U_{1,T} = h_0(-\mathbf{k}), \quad U_{1,C}^\dagger h_0^*(\mathbf{k}) U_{1,C} = -h_0(-\mathbf{k}).$$

These operators will also act on the tunneling matrix which must obey the same relation above. We now focus on the spin degrees of freedom as they play a crucial role in the form of the unitary operators and ultimate topological classification of the superconductor. We start by considering the unitary operators action on $h_0(\mathbf{k})$. With only a singlet component ($\hat{\Delta} = \hat{\Delta}_s$), the Hamiltonian will have full spin SU(2) symmetry, corresponding to a CI class with the time-reversal symmetry operator $\mathcal{T} = K$ and charge-conjugation given by $\mathcal{C} = \tau_2 K$. For a triplet superconductor ($\hat{\Delta} = \hat{\Delta}_t$), the d-vector defining the triplet order parameter characterizes the spin degrees of freedom. For our purposes, we will assume we the d-vector has a single component that breaks the SU(2) symmetry down into U(1) and leaves us in class AIII with time reversal $\mathcal{T} = is_2 K$ and charge conjugation $\mathcal{C} = \tau_1 K$.

We will now include perturbations to this Hamiltonian, some of which can be generated by an external field or an applied current (see below) that can be added to either $h_0(\mathbf{k})$ or $T(\mathbf{k})$ of the form

$$H_{\text{pert}}^{\alpha\beta}(\mathbf{k}) = \tau_\alpha (h_\beta(\mathbf{k}) s_\beta), \tag{11}$$

where $\alpha, \beta = 0, 1, 2, 3$ and $\mathbf{h}(\mathbf{k})$ is a spin and momentum dependent parameter corresponding to an external field. For our purposes, we consider each term independently, and we aim to find perturbations which

(1) preserve $\mathcal{T}$ and $\mathcal{C}$ in Eq. (9),
(2) open a gap in the spectrum,
(3) have a nontrivial topological index.

To satisfy condition (i) for a superconductor, we are automatically restricted to class DIII to form a $\mathbb{Z}_2$ invariant. Analyzing the possible perturbations under the discrete symmetries (see Appendix A) leads to the term

$$H_{\text{JSC}}(\mathbf{k}) = h(\mathbf{k}) \sigma_0 \tau_2 s_0, \tag{12}$$

that satisfies conditions (i) and (ii) so long as $h(\mathbf{k}) = -h(-\mathbf{k})$. Such a term can be considered as adding an ip component to the order parameter with d-vector component along s_2.

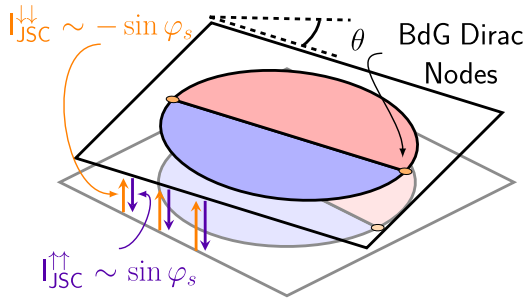

FIG. 3. Cartoon depiction a two nodal p wave superconductors rotated by an angle θ. The location of the Dirac nodes are denoted by orange dots. Interlayer spin current ($I^{\sigma\sigma}_{\rm JSC}$ where σ refers to the spin channel) results in a spin Josephson effect. Consequently, a rotation in spin space of the d-vector and Nambu space of the order parameter occurs which forms a $p_x + ip_y/p_x - ip_y$ order parameter.

Importantly, not all the momentum-odd character of Eq. (12) is consistent with Fermi-Dirac statistics. The effect of which results in differences for singlet and triplet superconductors. For a triplet superconductor, this term produces a helical order parameter while for singlet superconductors it violates Fermi-Dirac statistics. To amend this for singlet superconductors, such a term would require introducing a triplet order parameter which would produce a class AIII superconductor with a trivial topological classification in 2D [15]. The affect on a triplet order parameter, however, is allowed and sufficient to produce a class DIII superconductor. Starting with the two layer case, we show how such a component is generated by a Josephson spin current in triplet superconductors. To then satisfy condition (iii), we will compute a $\mathbb{Z}_2$ index which will be shown to depend on N and twist arrangement.

III. TOPOLOGICAL GAP OPENING WITH JOSEPHSON SPIN CURRENT

Before considering the stack of N layers, we first consider the effect of $H_{\rm JSC}(\mathbf{k})$ defined in Eq. (12) on the low-energy spectrum of a twisted bilayer:

$$H_2(\mathbf{k}) = \xi\tau_3 + \delta d_1(\mathbf{K}_N)\tau_1 s_3 - \alpha t d_1(\mathbf{K}_N)\tau_1\sigma_3 s_3 + t\tau_3\sigma_1, \tag{13}$$

where we take a triplet order parameter, and σ_i corresponds to the layer basis. Since all three rotation arrangements are equivalent for two layers, we take the layer to be rotated in opposing directions (incorporated in the σ_3 term) by a small angle $\pm\frac{\theta}{2}$. Compared to Eq. (8), the parameter α is halved due to half the rotation angle applied. The off-diagonal tunneling matrix is also captured by σ_1 and is given an explicit form of $T(\mathbf{k}) = t\tau_3$ which addresses the essential physical affects of twist while simplifying its form [10].

The application of the conventional charge (Josephson) supercurrent between layers induces a phase difference φ between the layers. This generates a term $\propto \tau_2$ in the low-energy Hamiltonian that breaks time reversal symmetry and opens a gap at the Dirac nodes [2,10]. Using the concept of the interlayer current, we can relate $H_{\rm JSC}(\mathbf{k})$ to an interlayer spin current illustrated in Fig. 3. Here, application of a pure spin current (which can be pictured as exactly compensated spin up and down components of Josephson charge current, see Fig. 3) leads to a misalignment of the d-vectors of the order parameters via a Josephson-like relationship (see Appendix C). Analogously to the application of an interlayer current, the order parameter will acquire a spin phase, i.e., with opposing signs for each spin channel such that $\Delta_1 \to \Delta_1(e^{i\varphi_s/2}s^{\uparrow\uparrow} + e^{-i\varphi_s/2}s^{\downarrow\downarrow})$ and $\Delta_2 \to \Delta_2(e^{-i\varphi_s/2}s^{\uparrow\uparrow} - e^{i\varphi_s/2}s^{\downarrow\downarrow})$ where $s^{\uparrow\uparrow} = \frac{s_0+s_3}{2}$ and $s^{\downarrow\downarrow} = \frac{s_0-s_3}{2}$. By using the current-phase relationship, we can represent the current of each spin channel as $I^{\sigma\sigma}(\Delta\varphi_s)$ where $\Delta\varphi_s$ is the spin-phase difference between the layers. The Josephson (spin) current I_{JC} ($I_{\rm JSC}$) is then the sum (difference) of the spin channels [33]. In the context of a Josephson junction, an applied spin current will induce a spin-dependent phase difference (φ_s) that generates a Josephson spin current. This realizes the spin Josephson effect, which is given by (see Appendix C)

$$I_{\rm JSC} = \frac{2t^2\nu_0}{\hbar}\sin(\varphi_s), \tag{14}$$

where ν_0 is the density of states at the Fermi energy. Since the phase difference for each spin channel is equal and opposite, the current (spin current) will be zero (nonzero). For a triplet superconductor, this acquired phase results in the transformation of the initially aligned d-vector to $\mathbf{d}(\mathbf{K}_N) = d_1(\mathbf{K}_N)(\cos\frac{\varphi_s}{2}, \sin\frac{\varphi_s}{2}, 0)$, resulting in the effective low-energy Hamiltonian $H_2(\mathbf{k}) \to \tilde{H}_2(\mathbf{k}) + H_{2,\rm JSC}(\mathbf{k})$, where

$$\tilde{H}_2(\mathbf{k}) = \xi\tau_3 + \delta\cos\frac{\varphi_s}{2}d_1(\mathbf{K}_N)\tau_1 s_3 - \alpha t\cos\frac{\varphi_s}{2}d_1(\mathbf{K}_N)\sigma_3\tau_1 s_3 + t\sigma_1\tau_3 \tag{15}$$

and

$$H_{2,\rm JSC}(\mathbf{k}) = -\delta\sin\frac{\varphi_s}{2}d_1(\mathbf{K}_N)\sigma_3\tau_2 + \alpha t\sin\frac{\varphi_s}{2}d_1(\mathbf{K}_N)\tau_2. \tag{16}$$

Note the latter term in $H_{2,\rm JSC}(\mathbf{k})$ corresponds to the gap-opening perturbation identified in Sec. II. Compared to the interlayer current, this spin current converts the Hamiltonian into a class DIII topological superconductor with helical edge modes of the form $p_x + ip_y/p_x - ip_y$. For singlet superconductors, the proposed mechanism of generating a TRI gap would not work, as the singlet order is even under $\mathbf{k} \to -\mathbf{k}$. However, the fermionic commutation relations imply that $H_{\rm JSC}(\mathbf{k})$ has to be odd in $\mathbf{k}$, or, in other words, will vanish identically if it is assumed to be even in $\mathbf{k}$. Moreover, applying a spin phase difference to an even order parameter can only generate even terms, and thus the term of interest will not be generated. Therefore opening a TRI gap in singlet SC would require the formation of a secondary spin triplet order parameter. Furthermore, if such a term is induced, it is insufficient to produce a stable $\mathbb{Z}_2$ invariant which is explored further in Appendix B and noted in Sec. II. Returning to the triplet scenario, if we take the spin current as small such that $\varphi_s \ll 1$, we can treat $H_{2,\rm JSC}(\mathbf{k})$ as a perturbation. The former term vanishes to first order and produces a negligible term of $\mathcal{O}(\varphi_s^2)$. Projected Eq. (13) and the latter term of Eq. (16) into the zero energy basis of Eq. (13), we find the effective Hamiltonian

$$\mathcal{H}_{\rm low}(\mathbf{k}) = -\tilde{\xi}\zeta_3\eta_3 - \tilde{\delta}\zeta_1\eta_3 - \tilde{m}\zeta_2\eta_0, \tag{17}$$

where ζ_i and η_j form our low-energy basis, $\tilde{\xi} = \sqrt{1-\alpha^2}\xi$, $\tilde{\delta} = \sqrt{1-\alpha^2}\delta$, and $\tilde{m} = \frac{t\alpha}{2}\varphi_s$. Each 2×2 block acts as a $p_x \pm ip_y$ superconductor which provide the helical counter-propagating edge modes.

We now aim to quantify the topological invariants of the Hamiltonian. A general approach is taken where we distinguish the eigenstates by diagonalizing them in the degenerate subspace with the $\hat{S}_z$ operator. For our two occupied states $|\nu_\alpha\rangle$ where $\alpha = \pm$, this amounts to diagonalizing the matrix

$$S_{\alpha,\beta} = |\nu_\alpha(k)\rangle\langle\nu_\alpha(k)|\sigma_z|\nu_\beta(k)\rangle\langle\nu_\beta(k)|. \tag{18}$$

The Chern number for the occupied eigenstates of the matrix can be computed as

$$C_\pm = \frac{1}{2\pi}\int d^2k Q_{K\pm}(k), \tag{19}$$

where [34]

$$Q_{K\pm}(k) = i(\langle\partial_{k_\parallel}\nu_\pm|\partial_{k_\perp}\nu_\pm\rangle - \langle\partial_{k_\perp}\nu_\pm|\partial_{k_\parallel}\nu_\pm\rangle). \tag{20}$$

Performing this calculation, we find $C_\pm = \pm\frac{\text{sign}(t\alpha\varphi_s)}{2}$. With these terms, we can recognize the spin Chern number $\mathcal{C}_s$

$$\mathcal{C}_s = C_+ - C_- = \text{sign}(t\alpha\varphi_s), \tag{21}$$

while the Chern number $\mathcal{C}$ is

$$\mathcal{C} = C_+ + C_- = 0. \tag{22}$$

The $\mathbb{Z}_2$ invariant can then be computed as the total spin Chern number by summing over all layers as each one contributes an additional node

$$\nu = \sum_i^N \mathcal{C}_s \mod 2 \equiv \mathcal{C}_{s,tot} \mod 2. \tag{23}$$

For the case of the two-layer Hamiltonian, this leads to a trivial $\mathbb{Z}_2$ index always, as the numbers of valleys, each containing two Dirac points, is even. Assuming each layer contributes a nonzero $\mathcal{C}_s$, we can naively expand this result to any layer number N where any even number of layers is topologically trivial, but opens the possibility of a nontrivial $\mathbb{Z}_2$ index for an odd number of layers. The complication with this general argument is that the twisting arrangements for more than two layers is not unique (see Fig. 1) and may affect the topology of the system. Using three layers as an example, we will consider several simple twisting arrangements to show when Eq. (23) can be applied to any N-layered system. In particular, we arrive at a nontrivial $\mathbb{Z}_2$ invariant for odd layered systems for CT and SLT set ups. We are then able to extend this result to N layers for the SLT cases.

IV. TRILAYER TWISTS

Given a spin current, the gap that is introduced provides a well-defined spin Chern number for a node. Although $\nu = 0$ for bilayers, an additional node in a trilayer system can provide $\nu = 1$ so long as the additional node becomes gapped. To express the Hamiltonian, we will start with Eq. (5) for $N = 3$ and assume the tunneling matrix $T = t\tau_3$ as in Sec. III resulting in

$$H_3(\mathbf{k}) = \begin{pmatrix} h_0(\mathbf{k}) & t\tau_3 s_0 & 0 \\ t\tau_3 s_0 & h_0(\mathbf{k}) & t\tau_3 s_0 \\ 0 & t\tau_3 s_0 & h_0(\mathbf{k}) \end{pmatrix}. \tag{24}$$

To introduce twists, we need to add the angle dependent terms of Eq. (8) corresponding to each twisting arrangement. Following the twisting orientations of Fig. 1, alternating twist (AT) will have twists applied in opposing orientations which leads to a twisting Hamiltonian

$$H_{\text{tw,AT}}(\mathbf{k}) = \sum_{n=1}^{N}(-1)^n\alpha d_1(\mathbf{K}_N)\tau_1 s_1\delta_{n,n}, \tag{25}$$

where $\delta_{n,n}$ is the Kronecker delta acting in layer space. Chiral twisting (CT) instead have the twist angle in the same orientation leading to a contribution

$$H_{\text{tw,CT}}(\mathbf{k}) = \sum_{n=1}^{N} n\alpha d_1(\mathbf{K}_N)\tau_1 s_1\delta_{n,n}. \tag{26}$$

For single-layer twisting (SLT), only a boundary layer is rotated while the other layers remain fixed which introduces a twisting Hamiltonian

$$H_{\text{tw,SLT}}(\mathbf{k}) = \alpha d_1(\mathbf{K}_N)\tau_1 s_1\delta_{n,1}, \tag{27}$$

where we chose the first layer as the rotated layer.

Each case behaves differently as α increases. For the case of ATs, the system can be treated as a bilayer and decoupled monolayer due to their different behavior under a mirror plane parallel to the layers [31,35,36]. As a result, an interlayer supercurrent only induces a gap for the coupled bilayer while the monolayer's nodes remain fixed. For CTs and SLTs, all layers are coupled where an interlayer supercurrent can gap all nodes in the layers producing a topological phase. One difference between the SLTs and the other two is that only ATs and CTs can achieve a magic angle at $\alpha_{\text{MA}} = \sqrt{2}$ marked by a quadratic and cubic band touching, respectively [31]. However, as Fig. 4 displays, SLTs form no band touching. Instead, at $\alpha = 0$, the nodes lie along $\delta = 0$ and as α starts to increase briefly causes the nodes along $k_\parallel$ to converge towards the center node. The node at the center then travels along $k_\perp$ away from the two nodes which remain fixed along $k_\parallel$. Further increasing α causes the single node to continue to travel further away along $k_\perp$.

The results for both CTs and SLTs have a convoluted analytical form, but we can obtain their response to an interlayer spin current numerically. Once a spin polarized spin difference is applied, the dispersion of both twist arrangements becomes gapped for $\alpha \neq 0$. Figure 5 shows how the gap energy evolves under increasing twist angle via α. For CTs, all nodes have the same gap energy which increases until $\alpha_{\text{MA}} = \sqrt{2}$ where it plateaus and then decreases as $\alpha > \sqrt{2}$. For SLTs, the gap energy is different between the center node and the pair of nodes along ξ. As α increases, the central node's gap energy exceeds the gap of the other two nodes. Regardless, the gaps follow the trajectory of the CTs' nodes albeit with smaller magnitude for all $\alpha > 0$.

To determine the topological invariant formed from the interlayer spin current, we focus on the SLT case (see Fig. 6)

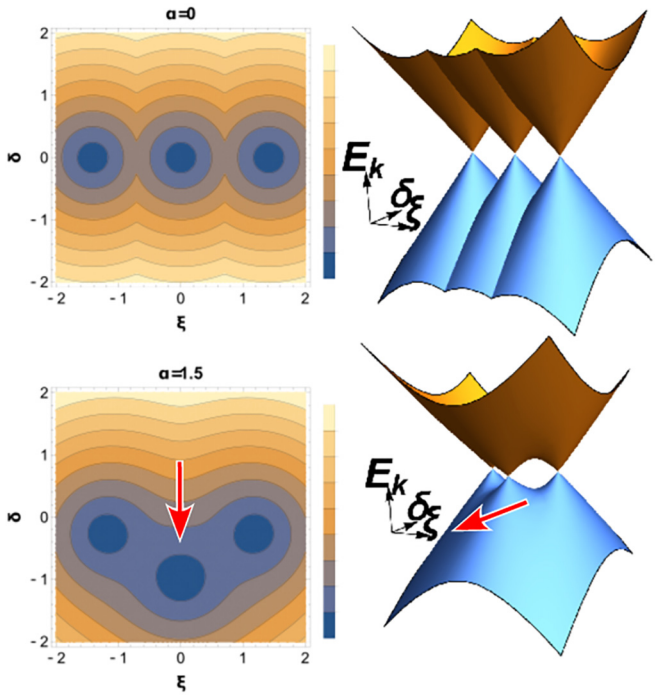

FIG. 4. Dispersion of the SLT Hamiltonian. For no twist ($\alpha = 0$), three nodes lie along ξ. As twist starts to increase, the nodes move together briefly. Afterwards, as shown when $\alpha = 1.5$, the central node moves away from the other two nodes along δ while the other nodes remain fixed. The red arrow depicts the direction the central node follows as α increases.

where we can treat the twist angle as small such that $\alpha \ll 1$. In this approximation, we start with an untwisted stack where the nodes lie along K_N. In doing so, the contribution of the order parameter and the twist along $k_\perp$ are perturbations about the zero energy eigenstates. The untwisted Hamiltonian can be represented by $\mathcal{H}_{\mathrm{SLT}}(\mathbf{k})$

$$\mathcal{H}_{\mathrm{SLT}}(\mathbf{k}) = \sum_{l=1}^{N=3} \Psi^\dagger_{\mathbf{k},l}\xi\tau_3\Psi_{\mathbf{k},l} + (\Psi^\dagger_{\mathbf{k},l-1}t\tau_3\Psi_{\mathbf{k},l} + \mathrm{H.c.}), \quad (28)$$

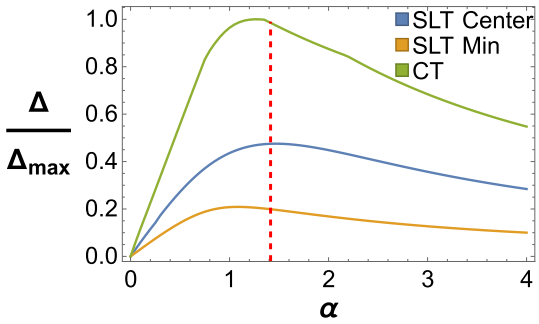

FIG. 5. Normalized gap energy vs α. For CTs, all nodes have the same gap which plateaus at $\alpha_{\mathrm{MA}} = \sqrt{2}$ highlighted by the red line. For SLTs, all nodes are gapped but with different magnitude. This difference is shown by the plots of the gap from the central node in blue and the minimum gap contributed by the remaining nodes in orange. Here, the gap energy is normalized by the maximum gap energy Δ_{max}, which is taken from the CTs' nodes.

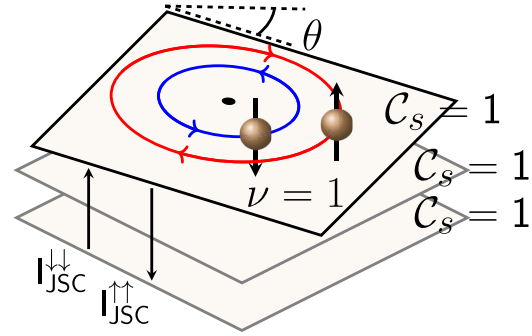

FIG. 6. Edge modes due to a finite $\mathbb{Z}_2$ index for the SLT trilayer system. For a SLT trilayer system with a interlayer spin current, a Dirac mass is introduced which forms a spin Chern number for each layer. Here $I^{\sigma,\sigma}$ represents the current spin channel of the order parameter. The BdG quasiparticles in brown can be given a helicity represented by the black arrows. These quasiparticles will form helical edge modes around impurities in the lattice. The corresponding $\mathbb{Z}_2$ formed by summing the spin Chern number provides a nontrivial index $\nu = 1$.

where $\Psi^\dagger_{\mathbf{k},l}$ are the same as discussed in Eq. (1). The zero energy eigenstates for this Hamiltonian can be written as a superposition of Bloch states using open boundary conditions for the layer hopping,

$$|\Psi^\dagger_{k_i^z}\rangle = \frac{1}{2}\sum_{l=1}^{N=3} \sin\left(k_i^z l\right)\Phi^\dagger_{\mathbf{k},l}|0\rangle, \quad (29)$$

where $\Phi^\dagger_{\mathbf{k},l}$ is a B-W spinor composed of $\Phi^\dagger_{\mathbf{k},l} = \Psi^\dagger_{\mathbf{k},l} - \Psi^\dagger_{\mathbf{k},-l}$. The momenta $k_i^z = \frac{i\pi}{4}$, $i = 1, 2, 3$ is oriented along the z direction which points perpendicular to the $(k_\parallel, k_\perp)$ plane along the stack of layers. The discrete index i comes from Fourier transforming the layers and therefore corresponds to the number of layers in the system.

We will now introduce a dispersion along $k_\perp$ which introduces a contribution from the order parameter as well as the interlayer spin current,

$$\mathcal{H}_\delta(\mathbf{k}) = \delta\sum_l \Psi^\dagger_{\mathbf{k},l}(\cos(\varphi_s l)\tau_1 s_3 - \sin(\varphi_s l)\tau_2 s_0)\Psi_{\mathbf{k},l}, \quad (30)$$

such that each layer has a phase $e^{i\varphi_s l}s^{\uparrow\uparrow} + e^{-i\varphi_s l}s^{\downarrow\downarrow}$ which ensures a phase difference between layers and opposing current in the spin channels. Applying the twist to the first layer adds a perturbation along the perpendicular direction,

$$\mathcal{H}_{tw}(\mathbf{k}, \varphi_s) = \alpha t\Psi^\dagger_{\mathbf{k},1}(\cos\varphi_s\tau_1 s_3 + \sin\varphi_s\tau_2 s_0)\Psi_{\mathbf{k},1}, \quad (31)$$

where the phase is incorporated from the spin current. Projecting these perturbations onto our low-energy basis, we find

$$\mathcal{H}_\delta\left(k_i^z\right) = \sum_{k_i^z} z_\delta\left(k_i^z\right)\Psi^\dagger_{k_i^z}(\cos(2\varphi_s)\tau_1 s_3 - \sin(2\varphi_s)\tau_2 s_0)\Psi_{k_i^z} \quad (32)$$

where

$$z_\delta\left(k_i^z\right) = \delta\frac{\cos^2\frac{\varphi_s}{2}\cos\varphi_s}{2\sin\left(k_z^i - \frac{\varphi_s}{2}\right)\sin\left(k_z^i + \frac{\varphi_s}{2}\right)}\sin^2 k_i^z \quad (33)$$

and

$$\mathcal{H}_{tw}(k_i^z) = \sum_{k_i^z} z_{tw}(k_i^z)\Psi^\dagger_{k_i^z}(\cos\varphi_s\tau_1 s_3 - \sin\varphi_s\tau_2 s_0)\Psi_{k_i^z}, \tag{34}$$

where

$$z_{tw}(k_i^z) = \frac{\alpha t}{2}\sin^2 k_i^z. \tag{35}$$

The low-energy effective Hamiltonian about each node then becomes

$$\mathcal{H}_{\text{eff}}(k_i^z) = \sum_{k_i^z} \Psi^\dagger_{k_i^z}\begin{pmatrix} \tilde{\xi}s_0 & \tilde{\delta}s_3 - i\tilde{m}s_0 \\ \tilde{\delta}s_3 + i\tilde{m}s_0 & -\tilde{\xi}s_0 \end{pmatrix}\Psi_{k_i^z}, \tag{36}$$

where $\tilde{\xi} = \xi - \xi_{k_i^z}$, $\tilde{\delta} = z_\delta(k_i^z)\cos(2\varphi_s) + z_{tw}(k_i^z)\cos\varphi_s$ and $\tilde{m} = z_\delta(k_i^z)\sin(2\varphi_s) + z_{tw}(k_i^z)\sin\varphi_s$.

Since the contribution of both twist and current to the Dirac mass is always $|\tilde{m}| > 0$, this leads to a well-defined Chern number. Furthermore, since $\tilde{\delta} > 0$ for all k_i^z, all gapped Dirac nodes will produce a Chern number with the same sign. Since the corresponding occupied eigenstates are orthogonal eigenstates of $\hat{S}_z$, we can evaluate the spin Chern number following Eq. (21) such that each node contributes

$$\mathcal{C}_s = \text{sign}(\alpha t \sin\varphi_s). \tag{37}$$

For this three layer case, we find $\mathcal{C}^{(3)}_{s,tot} \bmod 2 = 1$, leading to a stable $\mathbb{Z}_2$ index as illustrated in Fig. 6.

For SLTs we can now generalize this approach to N layers, allowing us to write the $\mathbb{Z}_2$ index as

$$\nu = \mathcal{C}^{(N)}_{s,tot} \bmod 2 = \sum_{l=1}^{N}\mathcal{C}_s \bmod 2$$
$$= \begin{cases} 0, & N \in 2\mathbb{N} \\ 1, & N \in 2\mathbb{N}+1 \end{cases}. \tag{38}$$

Thus, for the SLT geometry we are able to complete the computation of the $\mathbb{Z}_2$ index for N-layers spelled out in Eq. (23). On closer inspection of $z_\delta(k_i^z)$, when specifically choosing $\varphi_s = \frac{\pi}{2}$, this quantity vanishes. This result consequently marks a transition to new Dirac nodes appearing along $k_\perp$. Examined numerically, a pair of nodes appear at $k_2^z = \frac{\pi}{2}$ along $k_\perp$ leading to a total of three nodes at k_2^z. A more detailed investigation of current-driven generation of new Dirac nodes is provided in Ref. [32]. One consideration for these newly generated nodes is if they affect the $\mathbb{Z}_2$ invariant once formed. Because these new nodes are gapped and always introduced as pairs, their contribution will cancel and will have no affect on the $\mathbb{Z}_2$ invariant. Therefore Eq. (38) can be applied to any finite odd layered system and provide a nontrivial $\mathbb{Z}_2$ index.

V. DISCUSSION AND CONCLUSION

For N-layered twisted triplet nodal superconductors, we demonstrate how twist and spin current can produce a TRI topological phase. Starting with the AZ classifications on perturbations on a N-layer system, we identify one which is related to a Josephson spin current. With the Josephson spin current, we show that triplet twisted nodal superconductors transform its AZ classification to a DIII superconductor with a well-defined spin Chern number. This spin Chern number corresponds to a $\mathbb{Z}_2$ topological invariant which can be nontrivial for odd layered systems depending on the twisting arrangement, which is not unique.

To determine the influence of the twisting arrangement, we study a three layer system under common twisting configurations to show how chiral and single-layer twisting arrangements form a topological gap with an interlayer spin current. For the single-layer twists, we show with an effective low-energy model that this topological gap is accompanied by a nontrivial $\mathbb{Z}_2$ invariant. Extending into higher layer numbers where 2.5-D affects modify the distribution of Dirac nodes [32], the $\mathbb{Z}_2$ invariant remains nontrivial and can therefore be generalized to any odd layer number. Although a Josephson spin current hasn't presently been experimentally demonstrated, spin current measurements are well-known experimentally. This work represents a natural step forward in the general realization of topological superconductivity using twists and interlayer (spin) currents that now allow for a nontrivial $\mathbb{Z}$ or $\mathbb{Z}_2$ index.

While evidence of spin triplet superconductors in layered systems are not currently conclusive, many potential candidates are of current interest. Recent studies of trilayer rhombohedral graphene [37–39] have been suggested to host a f-wave order parameter, as well as potentially ZrNCl and WTe_2 serving as spin triplet platforms [40]. Our results may also provide a framework to continue this program of using stacking and twisting to realize higher order topological phases [41,42], which represents an interesting future direction. With advancements in finite size flakes of layered singlet superconductors, their extension to triplet superconductors and combination with spin current effects offer a future outlook for twisted superconducting systems.

ACKNOWLEDGMENTS

We thank Jennifer Cano, Marcel Franz, and Justin Wilson for useful discussions. This work is partially supported by NSF Career Grant No. DMR-1941569 and the Alfred P. Sloan Foundation through a Sloan Research Fellowship (K.L., J.H.P.). Part of this work was performed in part at the Aspen Center for Physics, which is supported by the National Science Foundation Grant No. PHY-2210452 (P.V., J.H.P.) as well as the Kavli Institute of Theoretical Physics that is supported in part by the National Science Foundation under Grants No. NSF PHY-1748958 and PHY-2309135 (P.V., J.H.P.).

APPENDIX A: PROJECTION OF TWO LAYER PERTURBATIONS

For two layers, we can write perturbations in the form $H^{\alpha\beta}_{\text{pert}}(\mathbf{k}) = \sigma_\alpha\tau_\beta(\mathbf{h}_\beta(\mathbf{k})\cdot\mathbf{s})$ where σ_i represents the layer basis and h is a parameter stemming, for example, from an external field. These perturbations are then applied to the two layer Hamiltonian in Eq. (13),

$$H_2(\mathbf{k}) = \xi\tau_3 + \delta d_1(\mathbf{K}_N)\tau_1 s_3 - \alpha t d_1(\mathbf{K}_N)\tau_1\sigma_3 s_3 + t\tau_3\sigma_1. \tag{A1}$$

TABLE I. Projections to the zero energy basis for allows terms of the form $\sigma_i\tau_j s_k$ with σ_i along the vertical axis and $\tau_j s_k$ along the horizontal. Here we assume that the perturbation is even under inversion.

	$\tau_3 s_0$	$\tau_3 s_1$	$\tau_2 s_2$
σ_0	$-\sqrt{1-\alpha^2}h\zeta_3$	$\sqrt{1-\alpha^2}h\eta_1$	—
σ_1	$h\zeta_3\eta_3$	$-h\eta_1$	—
σ_2	$h\alpha\zeta_1$	$-h\alpha\eta_2\zeta_1$	$-h\alpha\zeta_2\eta_2$
σ_3	$\alpha h\zeta_1\eta_3$	$2\alpha h\zeta_3\eta_3$	—

From the zero energy basis (represented by basis vectors η_i and ζ_i) of the two layer Hamiltonian, we can take perturbations which satisfy $\mathcal{C}$ and $\mathcal{T}$ and find their nonzero contribution via perturbation theory. For the case where $h(\mathbf{k}) = h(-\mathbf{k})$, these projections are summarized in Table I.

We can also consider the case when the perturbation is odd under inversion where $h(\mathbf{k}) = -h(-\mathbf{k})$. In this instance, several more terms are permitted which are presented for σ_i for $i \neq 2$ in Table II and σ_2 in Table III. Terms denoted by $(*)$ have no contribution to first order, so the presented terms are second order perturbations, and $\tilde{h} = h\sqrt{1-\alpha^2}$.

Let's highlight terms which may induce a Dirac mass. From the even terms, only $\sigma_2\tau_1 s_1$ may be considered. Examined numerically, for a sufficiently large value of h, a gap can open in the spectrum for $\alpha < \alpha_{\mathrm{MA}}$ (including zero) where the magic angle is shifted with the perturbation strength. After the magic angle, a nodal ring forms which then separates into two nodal rings which move away from one another along the perpendicular axis. The odd terms offer several possibilities which include those in the upper right of Table II:

- $\sigma_0\tau_2 s_0$, $\sigma_0\tau_3 s_2$, $\sigma_1\tau_2 s_0$, $\sigma_1\tau_3 s_2$.

From left to right, the first term $\sigma_0\tau_2 s_0$ corresponds to an equal spin current which opens a gap for all values of α. As analysis of this term shows, it can indeed be treated as a Dirac mass which produces a topological phase characterized by a spin Chern number. The second term $\sigma_0\tau_3 s_2$, however, forms nodal rings which then move towards and away from one another just as the nodal points in the unperturbed Hamiltonian. For the third term $\sigma_1\tau_2 s_0$, a gap opens for $\alpha < \alpha_{\mathrm{MA}}$ where the magic angle is shifted proportionally to the strength of the perturbation. Once the magic angle is reached, two Dirac nodes emerge and move along the perpendicular. The last term acts like the second term where nodal rings form for $\alpha < \alpha_{\mathrm{MA}}$. Except once the magic angle is reached, nodes form instead of rings with move along the perpendicular as the twist angle increases.

TABLE II. Projections to the zero energy basis for allows terms of the form $\sigma_i\tau_j s_k$ with σ_i for $i = 0, 1, 3$ along the vertical axis and $\tau_j s_k$ along the horizontal. Here we assume that the perturbation is odd under inversion.

	$\tau_0 s_1$	$\tau_0 s_3$	$\tau_1 s_1$	$\tau_1 s_3$	$\tau_2 s_0$	$\tau_3 s_3$
σ_0	$\tilde{h}\eta_2\zeta_2$	$-h\eta_3$	$-h\eta_1\zeta_3$	$\tilde{h}\zeta_1$	$h\zeta_2$	$-h\eta_1\zeta_2$
σ_1	$-h\eta_2\zeta_2$	$\tilde{h}\eta_3$	$\tilde{h}\eta_1\zeta_3$	$-h\zeta_1$	$-\tilde{h}\zeta_2$	$\tilde{h}\eta_1\zeta_2$
σ_3	$h\alpha\eta_1$	$\frac{h^2}{2t}\eta_3\zeta_3^*$	$-\frac{h^2}{2t}\eta_3\zeta_3^*$	$h\alpha\eta_3\zeta_3$	$-\frac{h^2}{2t}\eta_3\zeta_3^*$	$\frac{h^2}{2t}\eta_3\zeta_3^*$

TABLE III. Projections to the zero energy basis for allows terms of the form $\sigma_i\tau_j s_k$ with σ_i for $i = 2$ along the vertical axis and $\tau_j s_k$ along the horizontal for perturbations that are odd under inversion.

	$\tau_2 s_2$	$\tau_3 s_0$
σ_2	$-\frac{h^2}{2t}\eta_3\zeta_3^*$	$\frac{h^2}{2t}\eta_3\zeta_3^*$

APPENDIX B: SINGLET SUPERCONDUCTORS

Repeating the equal spin current analysis for a singlet superconductor likewise induces a spin phase. We will start by rewriting Eq. (1) for a two layer system to form the Block Hamiltonian $H_{2,s}(\mathbf{k})$,

$$H_{2,s}(\mathbf{k}) = \xi\tau_3 + \delta\tau_1 - \alpha t\sigma_3\tau_1 + t\tau_3\sigma_1, \tag{B1}$$

by absorbing the spin component into the BW spinor $\Psi_{\mathbf{k}} \to (is_2)\Psi_{\mathbf{k}}$. Applying the spin current transforms the Hamiltonian into $H_{2,s}(\mathbf{k}) \to \tilde{H}_{2,s}(\mathbf{k}) + H_{2,s,\mathrm{JSC}}(\mathbf{k})$

$$\tilde{H}_{2,s}(\mathbf{k}) = \xi\tau_3 + \delta\cos\frac{\varphi_s}{2}\tau_1 - \alpha t\cos\frac{\varphi_s}{2}\sigma_3\tau_1 + t\tau_3\sigma_1, \tag{B2}$$

$$H_{2,s,\mathrm{JSC}}(\mathbf{k}) = -\delta\sin\frac{\varphi_s}{2}\sigma_3\tau_2 s_3 + \alpha t\sin\frac{\varphi_s}{2}\tau_2 s_3. \tag{B3}$$

The imaginary component will break SU(2) symmetry but have a remaining quantization axis in spin space. As a result, this mechanism will transform the classification from CI to AIII but not produce a topological index. Another important remark is that the order parameter must also transform into a triplet in order to satisfy Fermi-Dirac statistics, so simply inducing a spin component to a singlet order parameter is insufficient. Therefore, in order to transform the classification for a singlet superconductor to DIII requires additional contributions. For example, for a d-wave superconductor, the order parameter must transform to $d \to d + ip$ (or another triplet order parameter), and lose the spin quantization with an additional Rashba spin-orbit coupling for example.

APPENDIX C: JOSEPHSON SPIN CURRENT IN TRIPLET SUPERCONDUCTORS

Here we demonstrate that for c-axis interface, spin current is related to a spin phase of the order parameter by a Josephson relation (for the planar case see Ref. [29]). Let us first define the charge (I_c) and spin (I_s) currents as

$$I_c = \frac{iet}{\hbar}\sum_{\mathbf{k},\sigma}[c^\dagger_{1,\sigma,\mathbf{k}}c_{2,\sigma,\mathbf{k}} - c^\dagger_{2,\sigma,\mathbf{k}}c_{1,\sigma,\mathbf{k}}]$$

$$= \frac{et}{\hbar}\sum_{\mathbf{k},\sigma}\Psi^\dagger_{\mathbf{k}}\sigma_2\Psi_{\mathbf{k}}, \quad I_s^{\alpha=1,2,3} = \frac{t}{\hbar}\sum_{\mathbf{k},\sigma}\Psi^\dagger_{\mathbf{k}}\sigma_2 s_\alpha\Psi_{\mathbf{k}}. \tag{C1}$$

We will now compute the currents perturbatively in the interlayer tunneling. This approach is sufficient at low twist angles, since the main contribution comes away from nodes [10]. In particular, we will consider here a p_x-wave order parameter $\hat{\Delta} \to \hat{\Delta}e^{i\varphi_s s_3\sigma_3/2}$: $\Delta_0\cos(\eta)\tau_1 s_3 \to \Delta_0\cos(\eta)[\cos(\varphi_s/2)\tau_1 s_3 + \sin(\varphi_s/2)\sigma_3\tau_2]$, where η is the angle on the Fermi surface. Note that such an operation is not possible for a singlet superconductor, since the spinful part of pairing has to be odd-parity. Consequently, application of a spinful phase difference to a singlet superconductor will result

in a renormalization of $\hat{\Delta}$ by $\cos(\varphi_s/2)$ only, while the spinful term will vanish identically due to fermion anticommutation.

Continuing with the z-polarized spin current, it is then given by

$$\begin{aligned} I_s^3 &= -\frac{it^2}{2\hbar} T \sum_{\varepsilon_n, \mathbf{k}} \mathrm{Tr}[\sigma_2 s_3 \hat{G}(i\varepsilon_n, \mathbf{k}) \sigma_3 \tau_1 \hat{G}(i\varepsilon_n, \mathbf{k})] \\ &= \frac{4t^2 \Delta_0^2 \sin(\varphi_s)}{\hbar} \int \frac{d\varepsilon d\mathbf{k}}{(2\pi)^3} \frac{\cos^2 \eta}{(\varepsilon^2 + \xi^2 + \Delta_0^2 \cos^2 \eta)^2} \Big|_{T=0} \\ &= \frac{2t^2 \nu_0 \sin(\varphi_s)}{\hbar}, \end{aligned} \tag{C2}$$

where ν_0 is the density of states and the factor of $1/2$ is to compensate for the summation over all the momentum space (rather than half due to extended spinor structure). Note that the final result is only valid at $T \ll \Delta_0$. In the case of $I_s^3 \neq 0$, the contribution from equal and opposite spin current will therefore results in no charge current.

Importantly, one can further demonstrate that all other components of spin current and charge current vanish. Therefore we have demonstrated that driving a spin current through a triplet twisted superconductor is equivalent to an application of spinful phase difference.

[1] O. Can, T. Tummuru, R. P. Day, I. Elfimov, A. Damascelli, and M. Franz, High-temperature topological superconductivity in twisted double-layer copper oxides, Nat. Phys. **17**, 519 (2021).

[2] P. A. Volkov, J. H. Wilson, K. P. Lucht, and J. H. Pixley, Current- and field-induced topology in twisted nodal superconductors, Phys. Rev. Lett. **130**, 186001 (2023).

[3] G. Margalit, B. Yan, M. Franz, and Y. Oreg, Chiral majorana modes via proximity to a twisted cuprate bilayer, Phys. Rev. B **106**, 205424 (2022).

[4] Y. Yu, L. Ma, P. Cai, R. Zhong, C. Ye, J. Shen, G. D. Gu, X. H. Chen, and Y. Zhang, High-temperature superconductivity in monolayer $Bi_2Sr_2CaCu_2O_{8+\delta}$, Nature (London) **575**, 156 (2019).

[5] P. A. Volkov, É Lantagne-Hurtubise, T. Tummuru, S. Plugge, J. H. Pixley, and M. Franz, Josephson diode effects in twisted nodal superconductors, Phys. Rev. B **109**, 094518 (2024).

[6] T. Tummuru, S. Plugge, and M. Franz, Josephson effects in twisted cuprate bilayers, Phys. Rev. B **105**, 064501 (2022).

[7] M. Martini, Y. Lee, T. Confalone, S. Shokri, C. N. Saggau, D. Wolf, G. Gu, K. Watanabe, T. Taniguchi, D. Montemurro, V. M. Vinokur, K. Nielsch, and N. Poccia, Twisted cuprate van der waals heterostructures with controlled Josephson coupling, Mater. Today **67**, 106 (2023).

[8] S. F. Zhao, X. Cui, P. A. Volkov, H. Yoo, S. Lee, J. A. Gardener, A. J. Akey, R. Engelke, Y. Ronen, R. Zhong *et al.*, Time-reversal symmetry breaking superconductivity between twisted cuprate superconductors, Science **382**, 1422 (2023).

[9] T. Tummuru, O. Can, and M. Franz, Chiral p-wave superconductivity in a twisted array of proximitized quantum wires, Phys. Rev. B **103**, L100501 (2021).

[10] P. A. Volkov, J. H. Wilson, K. P. Lucht, and J. H. Pixley, Magic angles and correlations in twisted nodal superconductors, Phys. Rev. B **107**, 174506 (2023).

[11] Y.-B. Liu, J. Zhou, Y. Zhang, W.-Q. Chen, and F. Yang, Making chiral topological superconductors from nontopological superconductors through large angle twists, Phys. Rev. B **108**, 064508 (2023).

[12] Y.-X. Li and C.-C. Liu, High-temperature majorana corner modes in a $d + id'$ superconductor heterostructure: Application to twisted bilayer cuprate superconductors, Phys. Rev. B **107**, 235125 (2023).

[13] C. Lin, C. Huang, and X. Lu, Customizing topological phases in the twisted bilayer superconductors with even-parity pairings, Chin. Phys. B **32**, 087401 (2023).

[14] A. Altland and M. R. Zirnbauer, Nonstandard symmetry classes in mesoscopic normal-superconducting hybrid structures, Phys. Rev. B **55**, 1142 (1997).

[15] A. P. Schnyder, S. Ryu, A. Furusaki, and A. W. W. Ludwig, Classification of topological insulators and superconductors in three spatial dimensions, Phys. Rev. B **78**, 195125 (2008).

[16] X.-L. Qi, T. L. Hughes, S. Raghu, and S.-C. Zhang, Time-reversal-invariant topological superconductors and superfluids in two and three dimensions, Phys. Rev. Lett. **102**, 187001 (2009).

[17] S. Ryu, A. P. Schnyder, A. Furusaki, and A. W. W. Ludwig, Topological insulators and superconductors: Tenfold way and dimensional hierarchy, New J. Phys. **12**, 065010 (2010).

[18] X.-L. Qi, T. L. Hughes, and S.-C. Zhang, Topological invariants for the Fermi surface of a time-reversal-invariant superconductor, Phys. Rev. B **81**, 134508 (2010).

[19] L. Fu and C. L. Kane, Superconducting proximity effect and majorana fermions at the surface of a topological insulator, Phys. Rev. Lett. **100**, 096407 (2008).

[20] S. Deng, L. Viola, and G. Ortiz, Majorana modes in time-reversal invariant s-wave topological superconductors, Phys. Rev. Lett. **108**, 036803 (2012).

[21] F. Zhang, C. L. Kane, and E. J. Mele, Time-reversal-invariant topological superconductivity and majorana kramers pairs, Phys. Rev. Lett. **111**, 056402 (2013).

[22] S. Qin, C. Fang, F.-C. Zhang, and J. Hu, Topological superconductivity in an extended s-wave superconductor and its implication to iron-based superconductors, Phys. Rev. X **12**, 011030 (2022).

[23] R.-X. Zhang and S. Das Sarma, Intrinsic time-reversal-invariant topological superconductivity in thin films of iron-based superconductors, Phys. Rev. Lett. **126**, 137001 (2021).

[24] J. Linder and J. W. Robinson, Superconducting spintronics, Nat. Phys. **11**, 307 (2015).

[25] F. S. Bergeret, A. F. Volkov, and K. B. Efetov, Odd triplet superconductivity and related phenomena in superconductor-ferromagnet structures, Rev. Mod. Phys. **77**, 1321 (2005).

[26] T. T. Heikkilä, M. Silaev, P. Virtanen, and F. S. Bergeret, Thermal, electric and spin transport in superconductor/ferromagnetic-insulator structures, Prog. Surf. Sci. **94**, 100540 (2019).

[27] Y. Zhi-Hong, Y. Yong-Hong, and W. Jun, Interfacial spin hall current in a Josephson junction with rashba spin-orbit coupling, Chin. Phys. B **21**, 057402 (2012).

[28] J. J. He, K. Hiroki, K. Hamamoto, and N. Nagaosa, Spin supercurrent in two-dimensional superconductors with rashba spin-orbit interaction, Commun. Phys. **2**, 128 (2019).
[29] Y. Asano, Josephson spin current in triplet superconductor junctions, Phys. Rev. B **74**, 220501 (2006).
[30] G. Rashedi and Y. Kolesnichenko, Spin polarized transport in the weak link between f-wave superconductors, Physica C: Superconductivity **451**, 31 (2007).
[31] T. Tummuru, E. Lantagne-Hurtubise, and M. Franz, Twisted multilayer nodal superconductors, Phys. Rev. B **106**, 014520 (2022).
[32] K. P. Lucht, J. H. Pixley, and P. A. Volkov, Topological superconductivity in twisted flakes of nodal superconductors, arXiv:2312.13367.
[33] Y. Mao and Q.-F. Sun, Spin phase regulated spin Josephson supercurrent in topological superconductor, Phys. Rev. B **105**, 184511 (2022).
[34] Y. Yang, Z. Xu, L. Sheng, B. Wang, D. Y. Xing, and D. N. Sheng, Time-reversal-symmetry-broken quantum spin hall effect, Phys. Rev. Lett. **107**, 066602 (2011).
[35] E. Khalaf, A. J. Kruchkov, G. Tarnopolsky, and A. Vishwanath, Magic angle hierarchy in twisted graphene multilayers, Phys. Rev. B **100**, 085109 (2019).
[36] L. Classen, J. Pixley, and E. J. König, Interaction-induced velocity renormalization in magic-angle twisted multilayer graphene, 2D Mater. **9**, 031001 (2022).
[37] H. Zhou, T. Xie, T. Taniguchi, K. Watanabe, and A. F. Young, Superconductivity in rhombohedral trilayer graphene, Nature (London) **598**, 434 (2021).
[38] Y.-Z. Chou, F. Wu, J. D. Sau, and S. Das Sarma, Acoustic-phonon-mediated superconductivity in rhombohedral trilayer graphene, Phys. Rev. Lett. **127**, 187001 (2021).
[39] B. T. Zhou, S. Egan, D. Kush, and M. Franz, Non-abelian topological superconductivity in maximally twisted double-layer spin-triplet valley-singlet superconductors, Commun. Phys. **6**, 47 (2023).
[40] V. Crépel and L. Fu, Spin-triplet superconductivity from excitonic effect in doped insulators, Proc. Natl. Acad. Sci. USA **119**, e2117735119 (2022).
[41] W. A. Benalcazar, B. A. Bernevig, and T. L. Hughes, Quantized electric multipole insulators, Science **357**, 61 (2017).
[42] F. Schindler, A. M. Cook, M. G. Vergniory, Z. Wang, S. S. Parkin, B. A. Bernevig, and T. Neupert, Higher-order topological insulators, Sci. Adv. **4**, eaat0346 (2018).